

Electronic Supplementary Information

Dative B←N bonds based crystalline organic framework with permanent porosity for acetylene storage and separation

Weize Wang,^{‡a} Linxia Wang,^{‡a} Fei Du,^a Gang-Ding Wang,^b Lei Hou,^{*b} Zhonghua Zhu,^c Bo Liu^{*a} and Yao-Yu Wang^b

^aCollege of Chemistry & Pharmacy, Northwest A&F University, Yangling 712100, P. R. China. E-mail: chemliubo@nwsuaf.edu.cn

^bKey Laboratory of Synthetic and Natural Functional Molecule of the Ministry of Education, Xi'an Key Laboratory of Functional Supramolecular Structure and Materials, College of Chemistry & Materials Science, Northwest University, Xi'an 710127, P. R. China. E-mail: lhou2009@nwu.edu.cn

^cSchool of Chemical Engineering, The University of Queensland, Brisbane, 4072, Australia.

[‡] These authors contributed equally.

Contents

Experimental section.....	S3
Materials and general methods	S3
Synthesis of BNOF-1	S3
Large-scale synthesis of BNOF-1	S3
Regeneration of BNOF-1	S3
Adsorption measurements.....	S4
GCMC simulation methodology.....	S4
Breakthrough experiments	S4
Molecular structures and physical properties of CO ₂ and C ₂ H ₂	S5
Powder X-ray diffraction (PXRD).....	S6
Thermogravimetric analysis (TGA).....	S6
PXRD patterns of BNOF-1 treated with different pH aqueous solutions.....	S7
PXRD patterns of BNOF-1 treated with different organic solvents	S7
Comparison of adsorption isotherms in different samples of BNOF-1	S8
Calculation of adsorption selectivity	S11
Calculation of adsorption heat (Q_{st}).....	S12
Fourier transform infrared spectroscopy (FT-IR)	S13
Comparison of adsorption performances and BET surface areas	S14
X-ray crystallography	S15
Summary of fitting parameters	S17
References.....	S18

Experimental section

Materials and general methods

All chemicals were purchased from commercial suppliers and used as received without further purification. Powder X-ray diffraction (PXRD) data were recorded on a Bruker D8 ADVANCE X-ray powder diffractometer (Cu K α , $\lambda = 1.5418 \text{ \AA}$). Thermogravimetric analysis (TGA) was carried out in a nitrogen stream using a Netzsch TG209F3 equipment at a heating rate of $10 \text{ }^\circ\text{C min}^{-1}$. Fourier transform infrared spectroscopy (FT-IR) measurement was performed on a Nicolet Avatar 360 FT-IR.

Synthesis of BNOF-1

The mixture containing 5 mg 4-pyridine boronic acid (PBA), 0.5 mL *N*-methylformamide (NMF), 0.5 mL MeCN and 120 μL HCOOH was sealed and ultrasound for 10 min in a vessel (10 mL). The vessel was heated to $120 \text{ }^\circ\text{C}$ for 12 h and then cooled to room temperature to give colorless rhombic crystals (yield: 70%, based on PBA). FT-IR: (KBr cm^{-1}): 3433 (w), 3313 (m), 3054 (m), 2866 (w), 2499 (w), 2359 (w), 1309 (m), 1675 (vs), 1624 (vs), 1535 (m), 1427 (vs), 1376 (vs, B–N), 1313 (vs), 1180 (vs), 1118 (m), 1058 (vs), 965 (vs), 841 (s) 779 (vs), 722 (vs), 644 (s), 588 (m), 445 (w) (Fig. S13).

Large-scale synthesis of BNOF-1

PBA (1.0 g), NMF (100 mL), MeCN (100 mL), and HCOOH (24 mL) were added into a 300 mL beaker and dissolved by ultrasound for 10 min. The solution was transferred to a 250 mL petri dish and kept in a $120 \text{ }^\circ\text{C}$ oven for 48 h. The colorless crystals (yield: $\sim 0.73 \text{ g}$) were produced at the bottom after cooling down to room temperature (Fig. 2a).

Regeneration of BNOF-1

Crystals of BNOF-1 were put in a 10 mL screw-cap vial containing NMF, and mixed

by ultrasound. The solution was clarified by heating at 160 °C, and then colorless crystals were recrystallized by slowly evaporating (Fig. 2b).

In addition, after being immersed in water for 1 h, the crystalline BNOF-1 was completely decomposed into the white precipitate PBA, which was collected by centrifugation, dried under vacuum, and can be reused to synthesize BNOF-1 through the same synthesis procedure (Fig. S3).

Adsorption measurements

The as-synthesized BNOF-1 was activated by heating at 433 K for 10 h under a dynamic vacuum. Adsorption measurements were performed on a Micrometrics ASAP 2020 Plus adsorption analyzer.

GCMC simulation methodology

All the Grand Canonical Monte Carlo (GCMC) simulations were performed for the gas adsorption in the framework by the Sorption module of Material Studio (Accelrys. Materials Studio Getting Started, release 5.0). The framework was considered to be rigid, and the gases were geometry optimized during the simulation. Partial charges for atoms of the guest-free framework were derived from Qeq method and QEq_neutral1.0 parameter. One unit cell was used during the simulations. The interaction energies between the gas molecules and framework were computed through the Coulomb and Lennard-Jones 6-12 (LJ) potentials. All parameters for the atoms were modeled with the universal force field (UFF) embedded in the MS modeling package. A cutoff distance of 12.5 Å was used for LJ interactions, and the Coulombic interactions were calculated by using Ewald summation. For each run, the 2×10^6 maximum loading steps, 2×10^6 production steps were employed.

Breakthrough experiments

The breakthrough experiment was performed on the Quantachrome dynaSorb BT equipments at 298 K and 1 bar with an equal volume of mixed gas (Ar as the carrier gas, flow rate = 5 mL min⁻¹). The activated BNOF-1 (0.6 g) was filled into a packed

column of ϕ 4.2 \times 80 mm, and then the packed column was washed with Ar at a rate of 7 mL min⁻¹ at 343 K for 60 min to further activate the samples. Between two breakthrough experiments, the adsorbent was regenerated by Ar flow of 7 mL min⁻¹ for 35 min at 353 K to guarantee complete removal of the adsorbed gases.

On the basis of the mass balance, the gas adsorption capacities can be determined as follows:

$$Q_i = \frac{C_i V}{22.4 \times m} \times \int_0^t \left(1 - \frac{F}{F_0}\right) dt$$

Where Q_i is the equilibrium adsorption capacity of gas i (mmol g⁻¹), C_i is the feed gas concentration, V is the volumetric feed flow rate (cm³ min⁻¹), t is the adsorption time (min), F_0 and F are the inlet and outlet gas molar flow rates, respectively, and m is the mass of the adsorbent (g).

		
Molecular size (Å ³)	3.18 \times 3.33 \times 5.36	3.32 \times 3.34 \times 5.7
Kinetic diameter (Å)	3.3	3.3
Boiling point (K)	194.7	189.3

Scheme S1. Molecular structures and physical properties of CO₂ and C₂H₂.

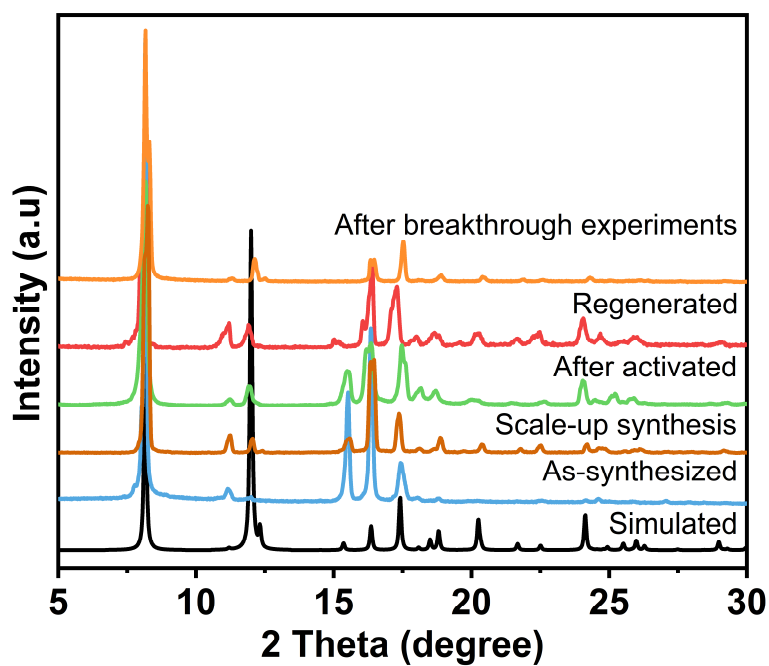


Fig. S1. PXRD patterns of BNOF-1 were obtained under different treated conditions.

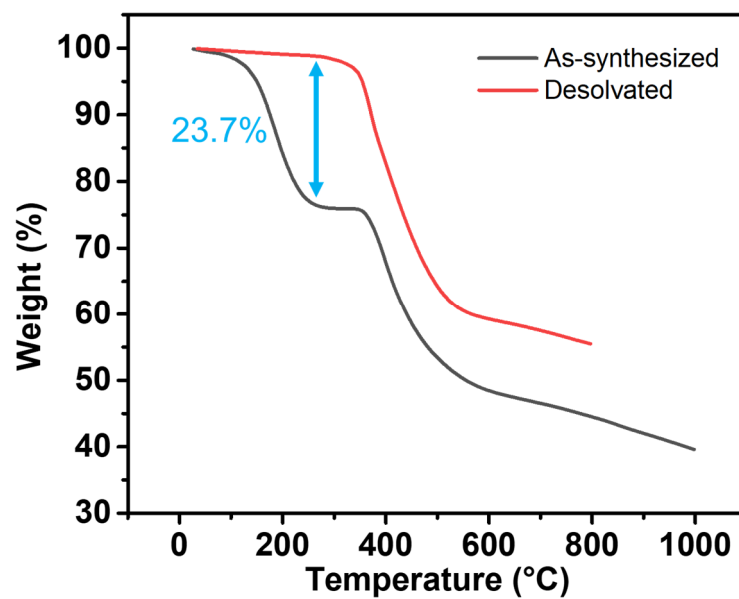


Fig. S2. TGA curves of BNOF-1.

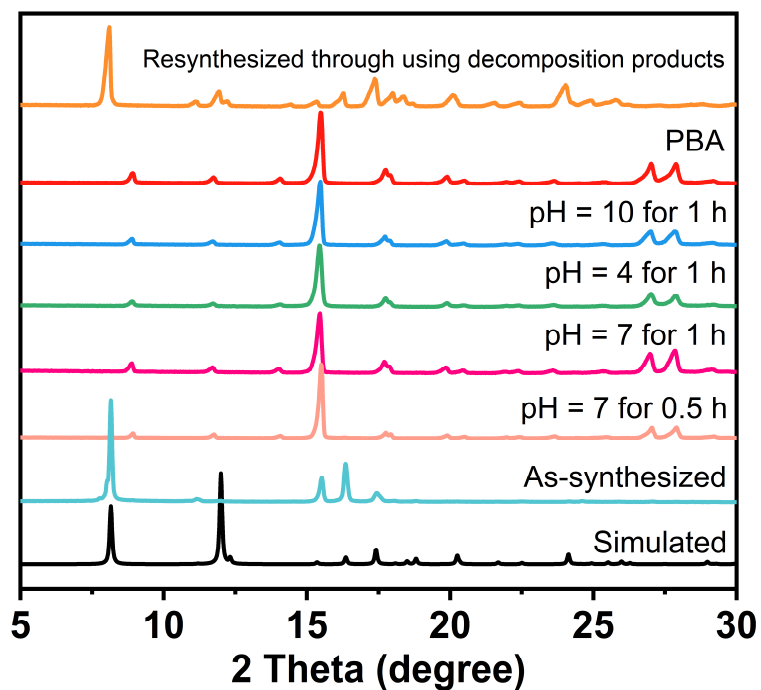


Fig. S3. PXRD patterns of PBA, BNOF-1 treated with different pH aqueous solutions, and resynthesized BNOF-1 through using PBA from the decomposition products.

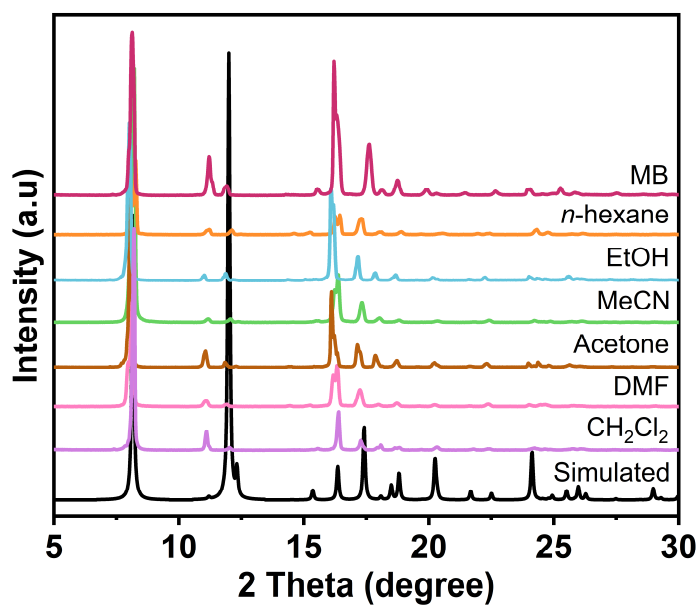


Fig. S4. PXRD patterns of BNOF-1 after immersing in various solvents for one week.

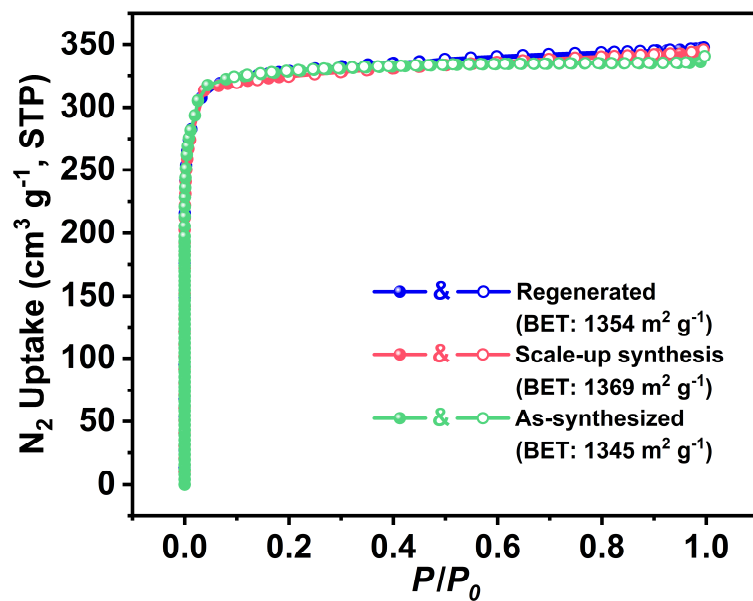


Fig. S5. Comparison of N₂ adsorption isotherms and BET surface areas at 77 K in different samples of BNOF-1.

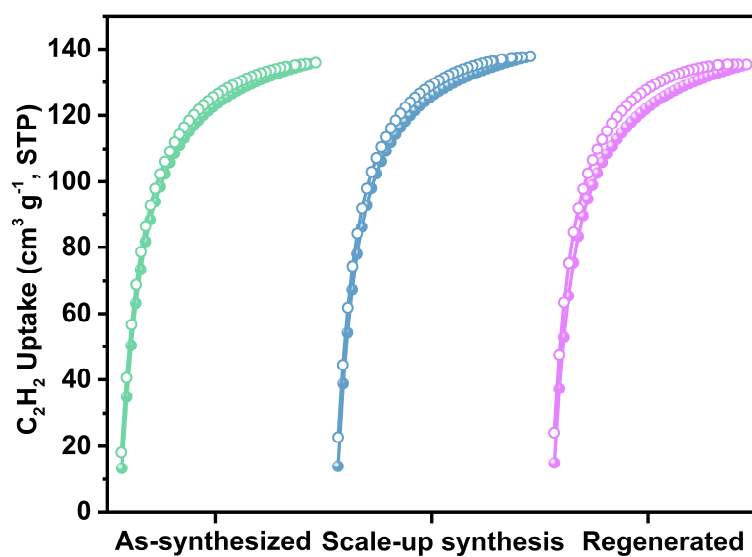


Fig. S6. Comparison of C₂H₂ adsorption isotherms at 273 K in different samples of BNOF-1.

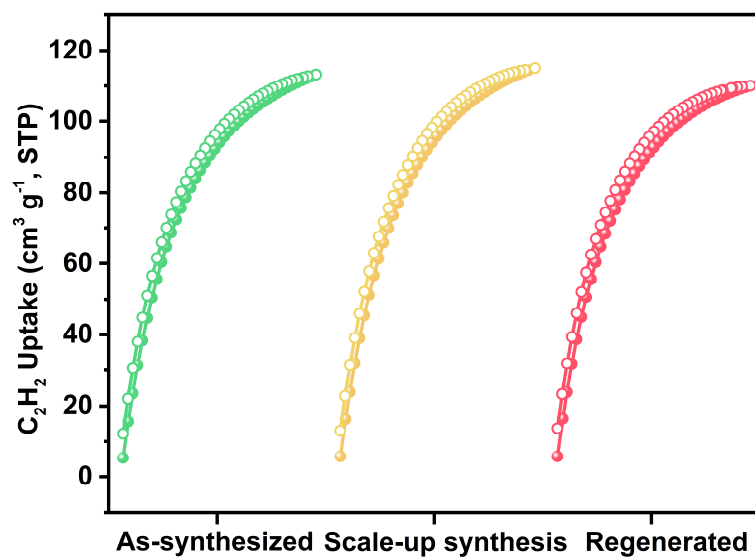


Fig. S7. Comparison of C₂H₂ adsorption isotherms at 298 K in different samples of BNOF-1.

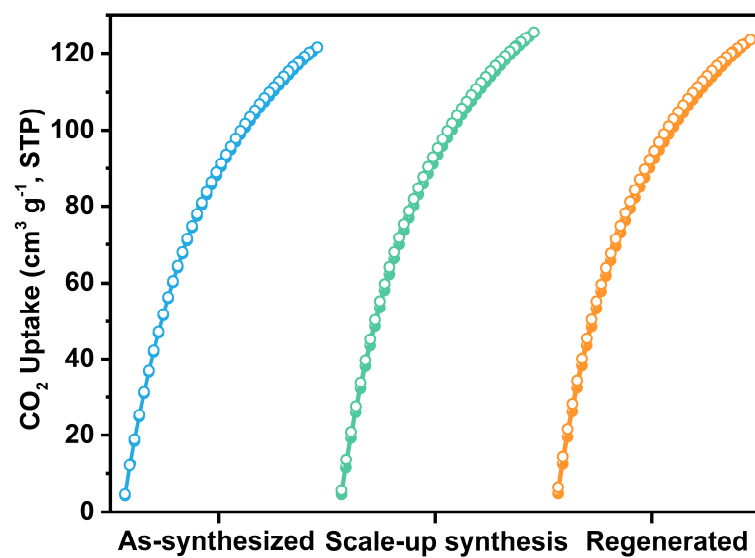


Fig. S8. Comparison of CO₂ adsorption isotherms at 273 K in different samples of BNOF-1.

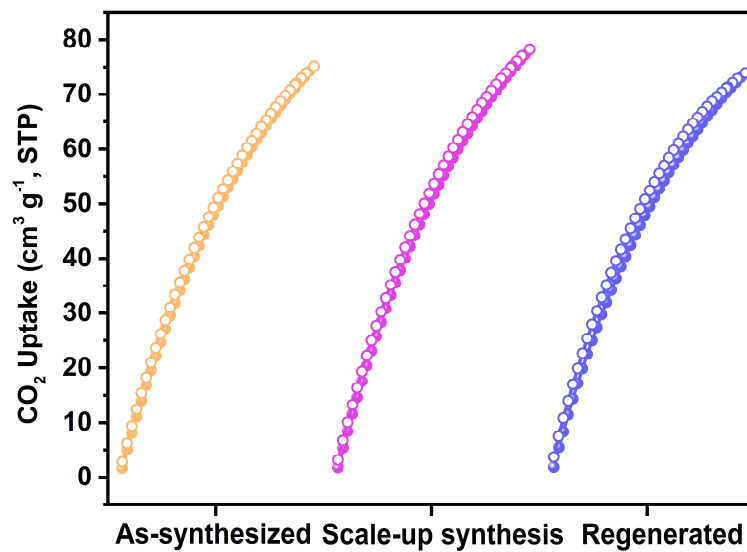


Fig. S9. Comparison of CO₂ adsorption isotherms at 298 K in different samples of BNOF-1.

Calculation of IAST adsorption selectivity

The experimental isotherm data for pure CO₂ and C₂H₂ (measured at 298 K) were fitted using a single-site Langmuir–Freundlich (L–F) model:

$$q = a_1 \frac{a_1 * b_1 * P^{c_1}}{1 + b_1 * P^{c_1}}$$

Where q and p are adsorbed amounts and pressures of component i , respectively.

The adsorption selectivity for binary mixtures of C₂H₂/CO₂ is defined by

$$S_{i/j} = \frac{x_i * y_j}{x_j * y_i}$$

were calculated using the Ideal Adsorption Solution Theory (IAST) of Myers and Prausnitz.

Where x_i is the mole fraction of component i in the adsorbed phase and y_i is the mole fraction of component i in the bulk.

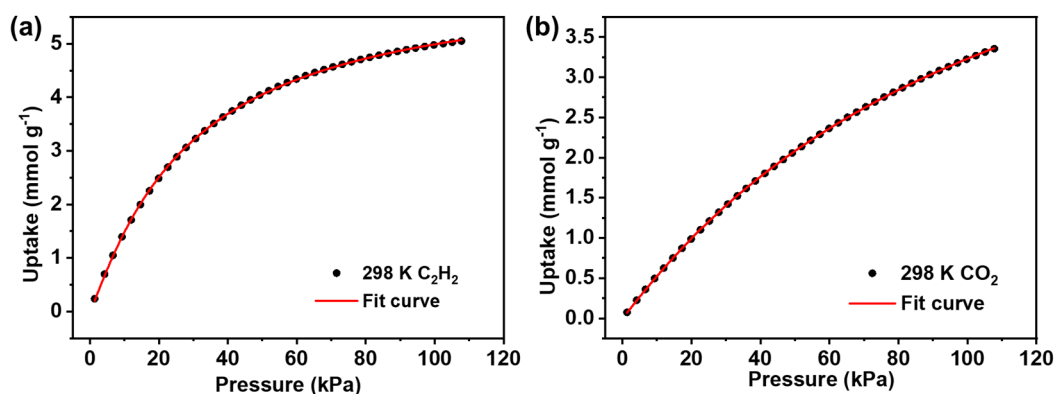


Fig. S10. (a) C₂H₂ and (b) CO₂ adsorption isotherms of BNOF-1 with fitting by the L–F model. Fitting results were given in Table S3.

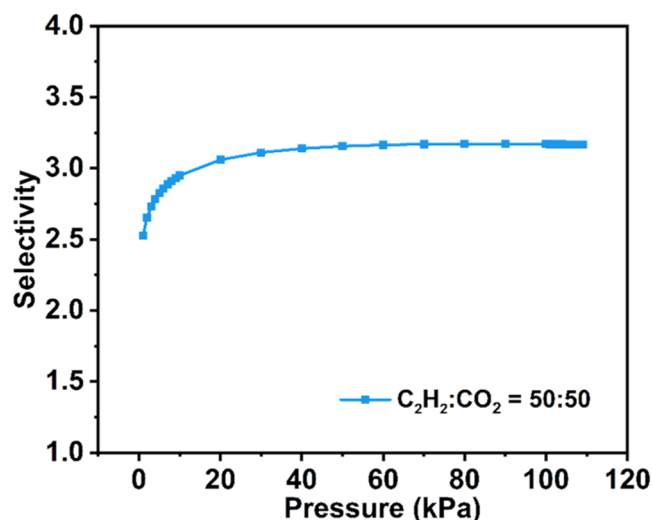


Fig. S11. Adsorption selectivity for equimolar C₂H₂-CO₂ mixtures calculated by IAST.

Calculation of sorption heat by using Virial II model

$$\ln(P) = \ln(N) + \frac{1}{T} \sum_{i=0}^m a_i N^i + \sum_{j=0}^n b_j N^j \quad Q_{st} = -R \sum_{i=0}^m a_i N^i$$

The above equation was applied to fit the combined gas isotherm data for BNOF-1 at 273 and 298 K, where P is the pressure, N is the adsorbed amount, T is the temperature, a_i and b_i are virial coefficients, and m and n are the number of coefficients used to describe the isotherms. Q_{st} is the coverage-dependent enthalpy of adsorption and R is the universal gas constant.

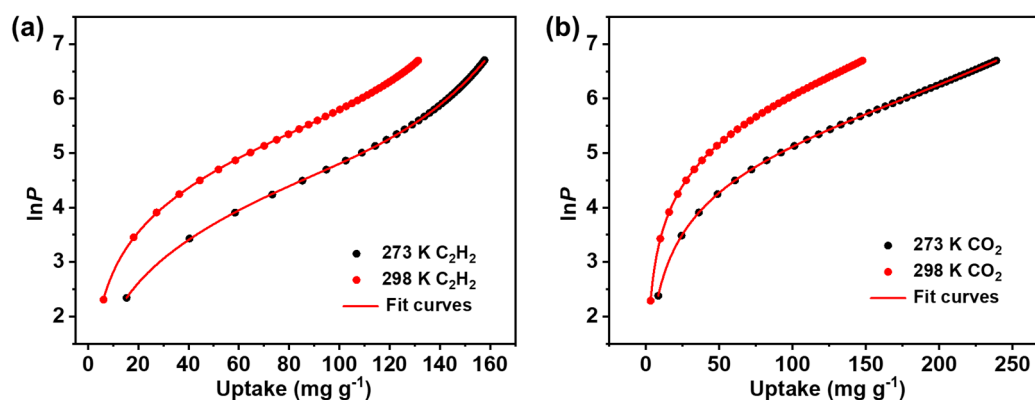


Fig. S12. Fitted adsorption isotherms for BNOF-1 with fitting by Virial II model. Fitting results were given in Table S4.

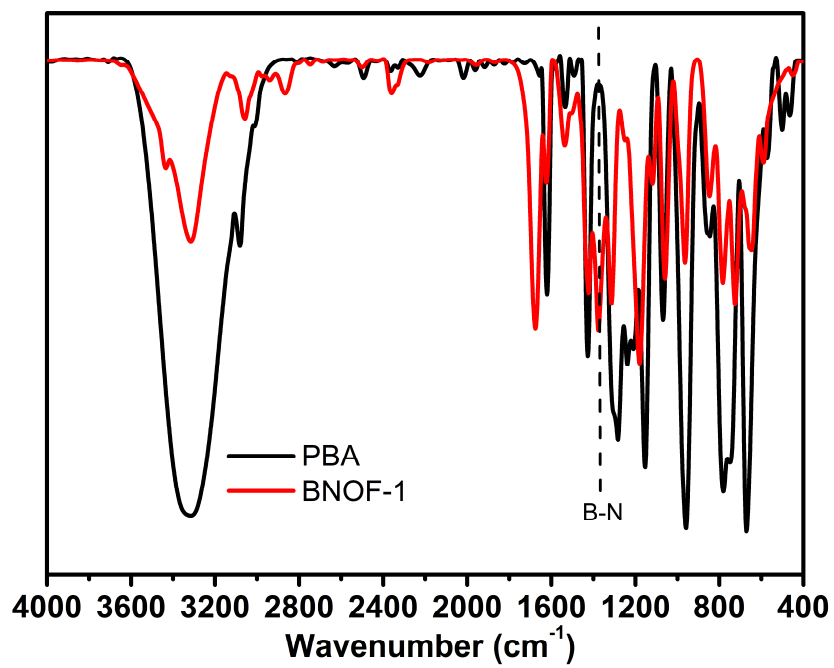


Fig. S13. IR spectra of BNOF-1 and PBA.

Table S1. Summary of adsorption capacity, Q_{st} , and BET surface area in reported COFs materials with C₂H₂/CO₂ separation performance.

Materials	C ₂ H ₂ (cm ³ g ⁻¹)	CO ₂ (cm ³ g ⁻¹)	Q_{st} (C ₂ H ₂ , kJ mol ⁻¹) ^[a]	BET (m ² g ⁻¹)	Ref.
BNOF-1	113.2 ^[b]	75.2 ^[b]	24.0	1345	This work
NKCOF-12	78 ^[b]	55 ^[b]	35.5	536	1
2D sqI COF	77.8 ^[b]	39.4 ^[b]	45.0	1048	2
3D pts COF	71.4 ^[b]	32.0 ^[b]	14.4	3738	
TpPa-NO ₂	63.73 ^[b]	45.18 ^[b]	42.57	398	3
PAF-120	50.8 ^[b]	30.0 ^[b]	37.5	801	4
NUS-72	48.0 ^[b]	11.2 ^[b]	30.1	720	5
NUS-71	42.4 ^[b]	10.3 ^[b]	32.7	582	
ZJUT-2	36.0 ^[b]	20.7 ^[b]	31.9	744	6
ZJUT-3	34.7 ^[b]	16.1 ^[b]	26.7	837	
H-AzoCOF	25 ^[c]	14 ^[c]	33.10	245	7
C ₁₀ -AzoCOF	18 ^[c]	9.0 ^[c]	32.64	29	
Tg-AzoCOF	17 ^[c]	7.6 ^[c]	34.01	28	

^[a]At zero coverage.

^[b]298 K, 1 bar.

^[c]295 K, 1 bar.

X-ray crystallography

Diffraction data were collected at 193 K with a Mo K α radiation ($\lambda = 0.71073 \text{ \AA}$) on a BrukerAXS SMART CCD area detector diffractometer. Absorption corrections were carried out utilizing SADABS routine. The structure was solved by the direct methods and refined using the SHELXTL program package. All non-hydrogen atoms were refined anisotropically with the hydrogen atoms added to their geometrically ideal positions and refined isotropically. The contribution of the disordered solvent molecules in the structure was subtracted from the reflection data by the SQUEEZE method as implemented in PLATON program. The final formula of BNOF-1 was determined by combining the single-crystal structures and TGA data. Data collection, structure refinement parameters and crystallographic data for BNOF-1 are given in Table S2.

Table S2. The crystallographic data of BNOF-1.

Name	BNOF-1
Empirical formula	C ₁₅ H ₁₂ B ₃ N ₃ O ₃
Formula weight	314.70
Temperature/K	193.0
Crystal system	orthorhombic
Space group	<i>Pmmn</i>
<i>a</i> /Å	11.4709(16)
<i>b</i> /Å	9.6054(15)
<i>c</i> /Å	10.811(2)
α /°	90
β /°	90
γ /°	90
Volume/Å ³	1191.1(3)
<i>Z</i>	2
<i>D</i> _{calc} (g cm ⁻³)	0.889
<i>F</i> (000)	328.0
Radiation	Mo K α (λ = 0.71073)
Reflections collected	6403
<i>R</i> _{int}	0.0902
Goodness-of-fit on <i>F</i> ²	1.063
<i>R</i> ₁ , ^a <i>wR</i> ₂ ^b [<i>I</i> > 2 σ (<i>I</i>)]	0.0764, 0.2276
<i>R</i> ₁ , ^a <i>wR</i> ₂ ^b [all data]	0.1181, 0.2564

$${}^a R_1 = \frac{\sum |F_o| - |F_c|}{\sum |F_o|}, \quad {}^b wR_2 = \left[\frac{\sum w(F_o^2 - F_c^2)^2}{\sum w(F_o^2)^2} \right]^{1/2}.$$

Table S3. Fitting results of CO₂ and C₂H₂ adsorption isotherms by L–F model.

	CO ₂	C ₂ H ₂
a ₁	6.84765	6.2365
b ₁	0.0077	0.02434
c ₁	1.03229	1.10812
Chi ²	1.17459E-5	1.65454E-4
R ²	0.99999	0.9999

Table S4. The fitting results of gas adsorption isotherms of BNOF-1 by Virial II model.

	CO ₂	C ₂ H ₂
b ₀	10.71424	9.85962
b ₁	0.00719	0.0587
b ₂	-1.84046E-5	-8.94017E-4
b ₃	4.12996E-7	5.15989E-6
a ₀	-2864.61173	-2790.8793
a ₁	-1.20485	-17.44339
a ₂	0.00461	0.31814
a ₃	-1.0528E-4	-0.00215
a ₄	4.25993E-9	2.96555E-6
Chi ²	5.55598E-7	4.32883E-5
R ²	1	0.99995

References

1. P. Zhang, Z. Wang, Y. Yang, S. Wang, T. Wang, J. Liu, P. Cheng, Y. Chen and Z. Zhang, *Sci. China Chem.*, 2022, **65**, 1173–1184.
2. L. Chen, C. Gong, X. Wang, F. Dai, M. Huang, X. Wu, C.-Z. Lu and Y. Peng, *J. Am. Chem. Soc.*, 2021, **143**, 10243–10249.
3. X.-H. Xiong, L. Zhang, W. Wang, N.-X. Zhu, L.-Z. Qin, H.-F. Huang, L.-L. Meng, Y.-Y. Xiong, M. Barboiu, D. Fenske, P. Hu and Z.-W. Wei, *ACS Appl. Mater. Interfaces*, 2022, **14**, 32105–32111.
4. L. Jiang, P. Wang, M. Li, P. Zhang, J. Li, J. Liu, Y. Ma, H. Ren and G. Zhu, *Chem.–Eur. J.*, 2019, **25**, 9045–9051.
5. Z. Zhang, C. Kang, S. B. Peh, D. Shi, F. Yang, Q. Liu and D. Zhao, *J. Am. Chem. Soc.*, 2022, **144**, 14992–14996.
6. C. Gong, H. Wang, G. Sheng, X. Wang, X. Xu, J. Wang, X. Miao, Y. Liu, Y. Zhang, F. Dai, L. Chen, N. Li, G. Xu, J. Jia, Y. Zhu and Y. Peng, *Angew. Chem., Int. Ed.*, 2022, **61**, e202204899.
7. S. Huang, Y. Hu, L.-L. Tan, S. Wan, S. Yazdi, Y. Jin and W. Zhang, *ACS Appl. Mater. Interfaces*, 2020, **12**, 51517–51522.